J Mater Sci: Mater Electron (2008) 19:687–691
DOI 10.1007/s10854-007-9380-8

Shallow and deep donors in n-type ZnO characterized by admittance spectroscopy

D. Seghier · H. P. Gislason

Received: 21 May 2007 / Accepted: 9 August 2007 / Published online: 8 September 2007

Abstract Shallow and deep energy levels in n-type ZnO materials grown by a pulsed laser injection method are investigated. We report thermal ionization energies for residual shallow donors of about E_d = 15 meV. Annealing in nitrogen ambient further lowers these ionization energies. We attribute these residual donors to native defects such as Zn interstitials and oxygen vacancies. Using optical admittance spectroscopy we also identify deep defects with optical ionization energies E_{o1} = 2.5 eV and E_{o2} = 2.1 eV. One of these centers is bistable with large capture barrier energy and therefore accounts for a significant part of the persistent photoconductivity in the material.

1 Introduction

ZnO has become very interesting for new applications in photonic and electronics because of the recent advances in bulk and epitaxial growth of this material [1, 2]. As-grown ZnO has a rather high density of free electrons the origin of which continues to be a topic of debate. Several ionization energies have been reported for the dominating shallow donors in ZnO [3]. Impurities such as Al, Ga and In are usually present in most ZnO crystals and can easily substitute for Zn ions and thus contribute to the conductivity [3]. However, hydrogen and native defects such as the zinc interstitial (Zn_i) and oxygen vacancy (V_O) have also been suggested to be significantly involved in the n-type conductivity [4]. Some authors have suggested that hydrogen could even be a dominating donor in ZnO [5]. In addition, the native defects Zn_i and V_O have also been reported to induce deep defects in the bandgap [6]. The high residual n-type conductivity in the material is a serious obstacle for obtaining high quality p-type ZnO. It is therefore necessary to investigate further the nature and origin of the residual n-type conductivity in ZnO, as well as the deep defects and their effect on the properties of the material.

In this work, we report investigations of ZnO materials using electrical and optically excited admittance aimed at contributing to the understanding of the conductance and the nature of point defects n-type ZnO.

2 Experimental procedure

High quality ZnO epilayers grown on c-sapphire substrates using pulsed laser injection from Nanovation were used in this study. Details about the growth technique are available elsewhere [7]. The thickness of the layers is about 200 nm. Hall measurements yield a free electron concentration of $n = 3 \times 10^{18}$ cm^{-3} and a mobility of μ_n = 300 cm^2/Vs at room temperature. For the electrical transport measurement Ti/Au alloys were evaporated onto the ZnO layer in order to obtain ohmic contacts. Selected samples were later subjected to annealing at 500 °C for 1 min in nitrogen ambient for comparison with the unannealed samples. Gold was evaporated onto the ZnO surface for making rectifying contacts. Impedance and admittance of the structures were determined with a Hewlett-Packard 4192A LF impedance analyzer, for frequencies in the range of 100 Hz to 1 MHz. The temperature range of investigation was from 80 K up to 400 K. A 100 W halogen lamp and a monochromator provided the monochromatic light used as the photoexcitation source.

D. Seghier (✉) · H. P. Gislason
Science Institute, University of Iceland, Dunhagi 3, 107 Reykjavik, Iceland
e-mail: seghier@hi.is

3 Results and discussion

Capacitance versus frequency (*C-f*) curves at three temperatures measured in an annealed sample are shown in Fig. 1. The measurements were performed at zero bias. All three curves exhibit the same behavior: the capacitance starts at a constant low-frequency value and drops by more than one order of magnitude before reaching the high-frequency range. The decrease in the capacitance occurs via two steps. At T = 120 K, for example, the cut-off frequencies for the two steps are at about $f = 1$ KHz and $f = 20$ kHz, respectively. The cut-off frequencies increase with temperature. *C-f* curves from both an annealed sample and an unannealed one are shown in Fig. 2 for comparison. The capacitance decrease in the unannealed sample occurs via only one step, with a cut-off frequency close to that of the first capacitance step in the annealed sample. Such a capacitance variation in both types of sample most likely reveals the presence of energy levels in the bandgap. Indeed, typical dispersion effects occur when the occupancy of an energy level is unable to follow a high-frequency voltage modulation and therefore cannot contribute to the net space charge in the depletion region. The *C-f* variations are well explained by capture and emission processes of electrons using the Shockley-Read-Hall statistics [8, 9].

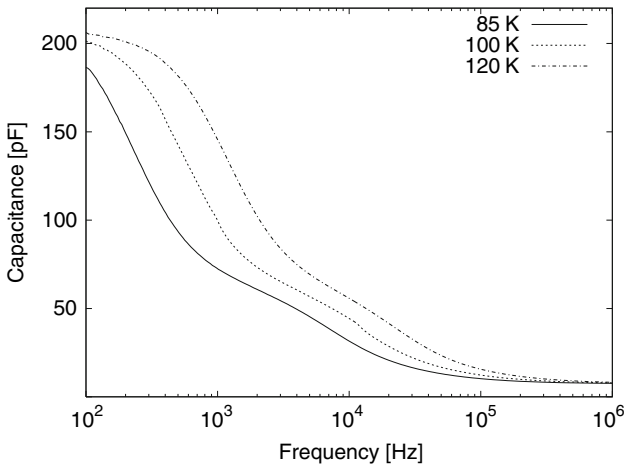

Fig. 1 Capacitance versus frequency at zero bias for three different temperatures measured in an annealed sample

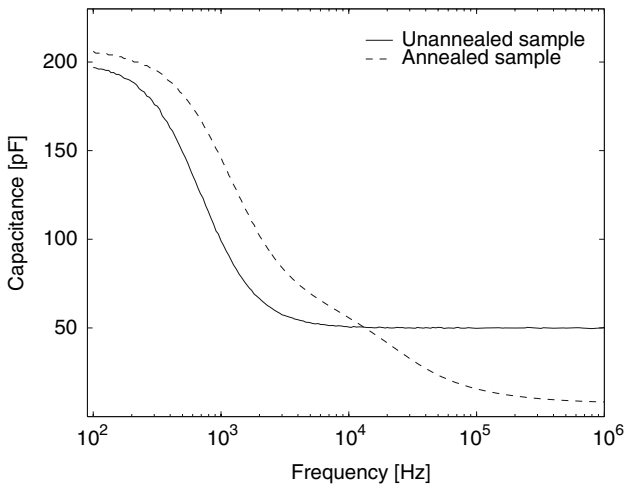

Fig. 2 Capacitance versus frequency. The dashed curve was measured in an annealed sample at 120 K and the solid curve in an unannealed sample at 120 K

As stated in the theory of admittance spectroscopy [10], a normalized conductance versus frequency (*G/f-f*) curve should exhibit a peak at the cutoff frequency of the *C-f* spectrum. Nevertheless, a high series resistance in the sample negatively affects the conductance, as has been reported in Ref. [11]. Therefore, it is likely that high series resistance in our materials explains why our *G/f-f* curves do not exhibit such peaks.

In order to determine accurately the cut-off frequencies of the capacitance we computed dC/d[ln(f)], the derivative of the capacitance with respect to the logarithm of the frequency, for the annealed sample as depicted in Fig. 3. As expected, two peaks are present in the annealed sample, A1 at lower and A2 at higher frequency, respectively. Only one peak U1 is observed in the unannealed one. A plot of $ln(f_0/T^2)$ versus 1/T provides the thermal activation energy and the capture cross section for the energy levels. We obtain the values $E_d = 15$ meV and $\sigma \approx 10^{-20}$ cm^2 for A1 and $E_d < 10$ meV and $\sigma \approx 10^{-20}$ cm^2 for A2. The same procedure yields an activation energy $E_d \approx 20$ meV and a capture cross section $\sigma \approx 3 \times 10^{-19}$ cm^2 for the U1 centre. The values for center U1 are rather close of those for center A1. In addition, a large dispersion in the capacitance caused by these defects suggests rather high densities for the centers, close to that of the shallow donors. Obviously center A1 has a higher concentration than center

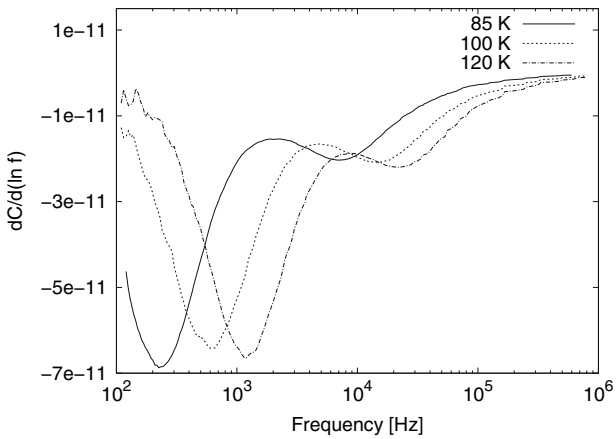

Fig. 3 dC/d[ln(f)] curves versus frequency measured at three different temperatures for an annealed sample

A2. From the very low thermal activation energies measured for these defect centers it is clear that they are shallow donors. Because of their high densities they must be the dominating donors in the material. Center A2 which is present only in the annealed sample is evidently produced by the annealing. Centers A1 and U1 most likely have the same origin. Also, annealing apparently changes the thermal activation energy of this donor slightly. Indeed, it is known that native defects in ZnO are mobile and sensitive to annealing even at low temperatures [12].

The origin of the residual n-type conductivity in ZnO is still a subject of debate. Kohan et al. concluded that Zn_i can be a shallow donor with high formation energy in ZnO [13]. However, Look et al. [14] showed that these centers can be involved in complex defects, which contribute significantly to the n-type conductivity and have rather low formation energies. Van de Walle, on the other hand, argued that hydrogen is the dominating shallow donor in ZnO [5]. SIMS measurements show that hydrogen is not present in a significant concentration in our samples [15]. Therefore, hydrogen is unlikely to be related to the shallow donors, which we observe. The high sensitivity of the donor ionization energy to annealing in our samples suggests that these centers are related to native defects such as Zn_i and V_O since these defects are known to be quite mobile. On the other hand, the average activation energy reported so far for shallow donors in ZnO mainly ranges between 30 and 60 meV. In our samples, which were grown by pulsed laser injection, we observe a much lower ionization energy, E_d = 15 meV. Also, annealing the samples in nitrogen ambient apparently results in a further lowering of the ionization energy of some of the donor centers to values as low as E_d = 10 meV. We are currently investigating annealings under various conditions in order to understand their effect on the n-type conductivity.

In Fig. 4 is shown an optical conductance spectrum from an annealed sample. Same measurements on the unannealed sample yield similar results. The material was illuminated with light of various wavelengths at room temperature. Appropriate filters were used each time to cut second order wavelengths from the excitation light. There are two maxima in the conductance spectrum of Fig. 4, one at 480 nm (2.5 eV) labeled O1 and another at 570 nm (2.1 eV) labeled O2. Maxima related to the bandgap absorption at 360 nm (3.4 eV) are not shown in the figure. The peaks are quite close to each other, but using higher resolution in the optical excitation did not further resolve them. According to the optical admittance theory [10] these conductance maxima are related to deep defects in the bandgap. Thus, the photon energies at which the maxima are observed are the optical ionization energies of the deep defects.

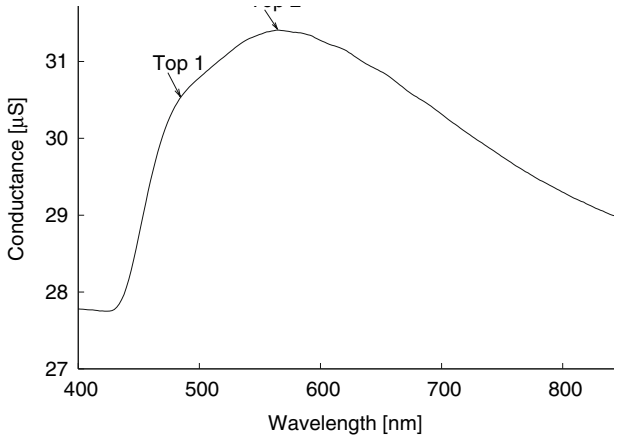

Fig. 4 Optical admittance spectrum measured at 300 K in an annealed sample

In order to investigate the admittance kinetics the annealed sample was illuminated at several temperatures with light of wavelength λ = 570 nm. This light wavelength corresponds to the energy associated with center O2. The photoconductance (PC) builds up to a saturation value, which is maintained as long as the excitation radiation is left on. The build-up rate is temperature dependant, slower at low temperatures. Below 200 K, for instance, it was not possible to reach a saturation value for the PC during illumination, even after waiting about one hour. The PC decay after the light is switched off is also strongly temperature dependent. Fig. 5 shows decay curves of the persistent PC at a few temperatures. The dark conductance has been subtracted from the curves in the figure and the values normalized to the maximum value obtained during illumination. After a decay time of 800 s the persistent PC is about 80% of its initial value at T = 260 K and at about 40% of its initial value at T = 320 K. When the sample is

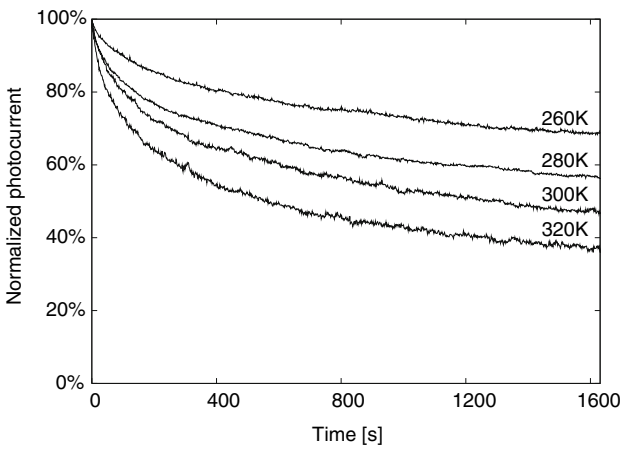

Fig. 5 Decay of the photoconductance after the excitation with light of wavelength • = 580 nm has been turned off at several temperatures for an annealed sample

illuminated with a light of wavelength $\lambda = 480$ nm very similar kinetics are obtained. However, when the wavelength of the illumination light is larger that 570 nm, that is with photon energy lower than 2.1 eV, a much weaker persistent PC is observed.

It is a common practice to fit data such that in Fig. 5 using a stretched exponential formula [16–18]:

$$G(t) = G_0 \exp[-(t/\tau)^{\beta}] \quad (1)$$

where $G(t)$ is the conductance at time t, G_0 the conductance at time $t = 0$, τ the decay time constant, and β the stretching factor. The values for τ are thermally activated and their temperature dependence can been fitted with the formula :

$$\tau = \tau_0 \exp(E_c/kT) \quad (2)$$

where E_c is the potential barrier for capture, τ_0 is the time constant without a potential barrier and T the temperature. The potential barrier for capture is obtained from an Arrhenius plot of $ln(\tau)$ as a function of $1/T$. A value of $E_c = 0.3$ eV was found for the center O2 as shown in Fig. 6.

So far, mainly electrical characterization techniques such as deep level transient spectroscopy (DLTS) have been applied to study electron traps in n-type ZnO [6, 19]. Therefore, most activation energies determined for such defects are thermal ones and range between 0.1 and 0.6 eV. We are not aware of other optical ionization energies for deep defects in ZnO than those reported here. From the slow decay transient of the PC after the illumination we conclude that center O2 is bistable. The high value of the capture barrier, $E_c = 0.3$ eV, associated with this center explains the related strong persistent PC, which persists even at room temperature. The fact that illumination with photon energy lower than 2.1 eV ($\lambda > 570$ nm) which does not photoionize O2, only induces a weaker persistent PC, implies that O2 is responsible for a significant part of the persistent PC of the material. It would be interesting to determine the thermal ionization energy for these centers in order to compare them to those reported in the literature. Unfortunately, it was not possible for us to perform DLTS on our samples as they were too highly conductive to be investigated by this technique. Due to the low density of incorporated hydrogen in our samples as deduced from SIMS measurements, we rule out the hypothesis that these centers are hydrogen-related. They are likely to be linked to complexes involving native defects in ZnO such as Zn_i and V_O.

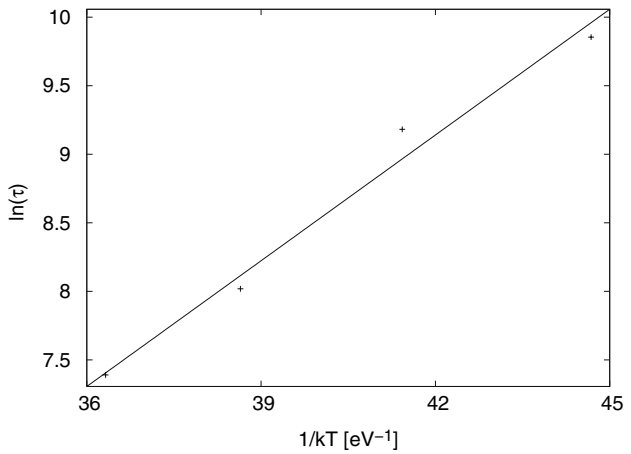

Fig. 6 Arrhenius plot of the photoconductivity decay lifetime • versus 1/T for the measurement in Fig. 4

4 Conclusion

We studied n-type ZnO layers grown by pulsed laser injection using electrical and optically excited admittance spectroscopy. We identified shallow energy levels with lower ionization energies than most values reported in the literature. In addition, annealing in nitrogen ambient seems to contribute to a further lowering of these ionization energies. We attribute the n-type conductivity in our samples to native defects in ZnO. Using optical admittance spectroscopy we identified two deep defects and measured their optical ionization energies. One of these centers was shown to be metastable and account for a large part of the persistent PC in the material. Further studies are in progress to identify the origin of these defects.

Acknowledgments We acknowledge S. A. Jonsson for assistance with the measurements. This research was supported by grants from the Icelandic Research Fund and the University of Iceland Research Fund. The authors thank Nanovation for providing the ZnO material and the EU SOXESS network for support.

References

1. D.C. Look, D.C. Reynolds, J.R. Sizelove, C.W. Litton, G. Cantwell, W.C. Harsch, Solid State Commun. **105**, 399 (1998)
2. B.K. Meyer, H. Alves, D.M. Hofmann, W. Kriegseis, D. Forster, F. Bertram, J. Christen, A. Hoffmann, M. Straßburg, M. Dworzak, U. Haboeck, A. V. Rodina, Phys. Status Solidi B **241**, 231 (2004)
3. Y. Natsume, H. Sakata, Mater. Chem. Phys. **78**, 170 (2002)
4. D.C. Look, J.W. Hemsky, J.R. Sizelove, Phys. Rev. Lett. **82**, 2552 (1999)
5. C.G. Van de Walle, Phys. Rev. Lett. **85**, 1012 (2000)
6. J.C. Simpson, J.F. Cordaro, J. Appl. Phys. **67**, 6760 (1990)
7. E.M. Kaidashev, M. Lorenz, H. von Wenckstern, A. Rahm, H.-C. Semmelhack, K.-H. Han, G. Benndorf, C. Bundesmann, H. Hochmuth, M. Grundmann, Appl. Phys. Lett. **82**, 3901 (2003).
8. W. Shockley, W.T. Read, Phys. Rev. **87**, 835 (1952).
9. R.N. Hall, Phys. Rev. **87**, 387 (1952).
10. P. Blood, J.W. Orton, *The Electrical Characterization of Semiconductors: Majority Carriers and Electron States* (Academic, London, 1992) p. 492

11. C. León, J.M. Martin, J. Santamaría, J. Skarp, G. González-Díaz, F. Sánchez-Quesada, J. Appl. Phys. **79**, 7830 (1996)
12. P. Erharta, K. Albe, Appl. Phys. Lett. **88**, 201918 (2006)
13. A.F. Kohan, G. Ceder, D. Morgan, C.G. Van de Walle, Phys. Rev. B 61, 15019 (2000)
14. D.C. Look, G.C. Farlow, P. Reunchan, S. Limpijumnong, S.B. Zhang K. Nordlund, Phys. Rev. Lett. **95**, 225502 (2005)
15. Nanovation, private communication
16. J.Y. Lin, A. Dissanayake, H.X. Jiang, Solid State Commun. **87**, 787 (1993)
17. J.Y. Lin, A. Dissanayake, G. Brown, H.X. Jiang, Phys. Rev. B. **42**, 5855 (1990)
18. A. Dissanayake, S.X. Huang, H.X. Jiang, J.Y. Lin, Phys. Rev. B. **44**, 13343 (1991)
19. F.D. Auret, S.A. Goodman, K.J. Legodi, E. Meyer, D.C. Look, Appl. Phys. Lett. **80**, 1340 (2002)